Charge qubit dynamics in a double quantum dot coupled to phonons

Zhuo-Jie Wu,* Ka-Di Zhu, Xiao-Zhong Yuan, Yi-Wen Jiang, and Hang Zheng
Department of Physics, Shanghai Jiao Tong University, Shanghai 200240, China
(Received 18 December 2004; revised manuscript received 21 March 2005; published 31 May 2005)

The dynamics of charge qubit in a double quantum dot coupled to phonons is investigated theoretically in terms of a perturbation treatment based on a unitary transformation. The dynamical tunneling current is obtained explicitly. The decoherence induced by acoustic phonons is analyzed in detail after a derivation of spectral density. It is shown that the contribution from deformation potential coupling is comparable to that from piezoelectric coupling in small dots and large tunneling rates. A possible decoupling mechanism is predicted.

DOI: 10.1103/PhysRevB.71.205323 PACS number(s): 73.23.Hk, 73.63.Kv, 03.65.Yz, 03.67.Lx

I. INTRODUCTION

Computers based on quantum mechanics are proven to be more efficient in some specific calculations than those based on classical physics.[1–3] The first step to build a quantum computer is the realization of the building block called quantum bit (qubit). Within the last decade, various schemes have been proposed and many of them have even been realized.[4–8] Among them, the electrically controlled charge qubit in a semiconductor double quantum dot has the potential advantages of being arbitrarily scalable to large system and compatible with the current microelectronics technology. Besides, the double-dot system is also extremely useful in basic physics as it enables us to investigate the decoherence and dissipation of a small quantum system interacting with its environment.

Various designs of double-dot qubits have been studied in experiments.[9–12] Recently, Hayashi *et al.* have successfully realized coherent manipulation of electronic states in a double-dot system implemented in a GaAs/AlGaAs heterostructure containing a two dimensional electron gas. The damped Rabi oscillation is observed in the time domain in their experiment and an empirical formula is presented to fit the experimental data.[13] Fujisawa *et al.* explain the transport in this system through density matrix simulations.[14] But the phonon effects are not included. However, the phonon induced decoherence is significant according to the analysis of Ref. 13. Considering the interaction with the piezoelectric acoustic phonons, Brandes *et al.* have investigated in detail the single electron tunneling in a double quantum dot.[15–19] Fedichkin and Fedorov also study the error rate of the charge qubit coupled to an acoustic phonon reservoir.[20,21] But no dynamical tunneling current is presented by all these works. In a latest review paper,[22] Brandes derives the dynamical tunneling current in the weak electron-phonon dissipation limit through Born-Markov approximation, but the result is rather complicated.

In this work, we study the damped Rabi oscillation observed in Ref. 13. The quantum dynamics of a single electron tunneling in the double-dot system is investigated without applying the Born-Markov approximation to the electron-phonon interaction. A simple explicit expression of dynamical tunneling current is presented through perturbation treatment based on a unitary transformation. The phonons (both the deformation potential and piezoelectric contribution are included) induced decoherence are investigated in detail and possible decoupling mechanism is presented.

This paper is organized as follows. In Sec. II we introduce the model Hamiltonian for the charge qubit and solve it in terms of a perturbation treatment based on a unitary transformation. The spectral density is derived in Sec. III. In Sec. IV, we analyze the phonon induced decoherence. Finally, the conclusion is given in Sec. V.

II. MODEL AND THEORY

In this section, we shall introduce the model Hamiltonain for the double quantum dot and then develop general theory leading to explicit expression for the dynamical current. We will focus on the phonon effect on the qubit dynamics.

A. Model Hamiltonian

The double quantum dot consists of left and right dots connected through an interdot tunneling barrier. Due to Coulomb blockade, only one excess electron is allowed to occupy the left or right dot, which defines two basis vectors $|L\rangle$ and $|R\rangle$ (with the energy level ε_L and ε_R, respectively) in Hilbert space. The energy difference between these two states $\varepsilon=\varepsilon_L-\varepsilon_R$ can be controlled by the source-drain voltage V_{sd}.[13] Considering the coupling to its environment, the double dot can be described by the Hamiltonian,

$$H = H_e + H_p + H_{ep} + H_r + H_{er}, \tag{1}$$

where the qubit Hamiltonian reads ($\hbar=1$)

$$H_e = -\tfrac{1}{2}\varepsilon(t)\sigma_z + T_c\sigma_x, \tag{2}$$

where T_c is the interdot tunneling, σ_x and σ_z are Pauli matrix with $\sigma_z=|L\rangle\langle L|-|R\rangle\langle R|$ and $\sigma_x=|L\rangle\langle R|+|R\rangle\langle L|$. If the qubit isolates from any other degrees of freedom, the excess electron would oscillate coherently between two dots with the Rabi frequency $\Delta=\sqrt{\varepsilon^2+4T_c^2}$. However, the qubit must couple to its environment (phonons and electron reservoir in leads) in practice. H_p and H_{ep} stand for the phonon reservoir and its coupling to charge qubit, respectively. They can be written as follows:

$$H_p = \sum_{\mathbf{q},\lambda} \omega_{\mathbf{q},\lambda} b^\dagger_{\mathbf{q},\lambda} b_{\mathbf{q},\lambda}, \tag{3}$$

$$H_{ep} = \frac{1}{2}\sigma_z \sum_{\mathbf{q},\lambda} (M_{\mathbf{q},\lambda} b^\dagger_{\mathbf{q},\lambda} + M^*_{\mathbf{q},\lambda} b_{\mathbf{q},\lambda}), \tag{4}$$

where $b^\dagger_{\mathbf{q},\lambda}$ ($b_{\mathbf{q},\lambda}$) and $\omega_{\mathbf{q},\lambda}$ are the creation (annihilation) operators and energy of the phonons with the wave vector $\mathbf{q}$ and polarization λ, respectively, $M_{\mathbf{q},\lambda}$ is the electron-phonon coupling constant. The effects of the phonon bath are fully described by a spectral density

$$J(\omega) = \sum_{\mathbf{q},\lambda} |M_{\mathbf{q},\lambda}|^2 \delta(\omega - \omega_{\mathbf{q},\lambda}). \tag{5}$$

H_r and H_{er} in the Hamiltonian H stand for the electron reservoir in leads and its coupling to charge qubit, respectively.

In experiment, a pulse technique is used to switch the V_{sd} from large bias in the initialization process (an excess electron localizes in the left dot) to the zero bias in the manipulation process [the double dot is isolated from leads, and the excess electron tunnels resonantly (i.e., $\varepsilon = 0$) back and forth between two dots].[13] Restoring a large bias voltage V_{sd} after the pulse time t it gives the measurement of dynamical elastic tunneling current which is described by the probability $n(t)$ of the excess electron in the right dot at that exact time.

Neglecting the higher order tunneling (cotunneling) between leads and the dots, the effective Hamiltonian in the manipulation process reads

$$H_{\text{eff}} = T_c \sigma_x + \sum_{\mathbf{q}} \omega_{\mathbf{q}} b^\dagger_{\mathbf{q}} b_{\mathbf{q}} + \frac{1}{2}\sigma_z \sum_{\mathbf{q}} (M_{\mathbf{q}} b^\dagger_{\mathbf{q}} + M^*_{\mathbf{q}} b_{\mathbf{q}}). \tag{6}$$

Here, for the sake of simplicity, we omit the polarization, since it makes no difference in the theory below. When it makes difference (in Sec. IV), it will be included again. This effective Hamiltonian is the starting point of our theory.

B. Theory

The effective Hamiltonian H_{eff} is equivalent to the spin-boson Hamiltonian in zero bias case. Though it seems rather simple, it cannot be solved exactly. Various analytical or numerical approaches have been proposed to obtain an approximate solution to it.[23,24]

Here, we apply a canonical transformation, $H' = \exp(S) H_{\text{eff}} \exp(-S)$, with the generator,[25–27]

$$S = \sum_{\mathbf{q}} \frac{\xi_{\mathbf{q}}}{2\omega_{\mathbf{q}}} (M_{\mathbf{q}} b^\dagger_{\mathbf{q}} - M^*_{\mathbf{q}} b_{\mathbf{q}}) \sigma_z. \tag{7}$$

Thus we get the Hamiltonian H', and decompose it into $H' = H'_0 + H'_1 + H'_2$, where

$$H'_0 = \eta T_c \sigma_x + \sum_{\mathbf{q}} \omega_{\mathbf{q}} b^\dagger_{\mathbf{q}} b_{\mathbf{q}} - \sum_{\mathbf{q}} \frac{|M_{\mathbf{q}}|^2}{4\omega_{\mathbf{q}}} \xi_{\mathbf{q}} (2 - \xi_{\mathbf{q}}), \tag{8}$$

$$H'_1 = \frac{1}{2}\sigma_z \sum_{\mathbf{q}} (1 - \xi_{\mathbf{q}})(M_{\mathbf{q}} b^\dagger_{\mathbf{q}} + M^*_{\mathbf{q}} b_{\mathbf{q}}) + \eta T_c i\sigma_y A, \tag{9}$$

$$H'_2 = T_c \sigma_x (\cosh A - \eta) + T_c i\sigma_y (\sinh A - \eta A), \tag{10}$$

where

$$A = \sum_{\mathbf{q}} \frac{\xi_{\mathbf{q}}}{\omega_{\mathbf{q}}} (M_{\mathbf{q}} b^\dagger_{\mathbf{q}} - M^*_{\mathbf{q}} b_{\mathbf{q}}), \tag{11}$$

and η is a parameter which will be adjusted to minimize the perturbation terms (H'_1 and H'_2). Obviously, H'_0 can be solved exactly. We denote the ground state of H'_0 as

$$|g\rangle = |s_2\rangle |\{0_{\mathbf{q}}\}\rangle, \tag{12}$$

and the lowest excited states as

$$|e_s\rangle = |s_1\rangle |\{0_{\mathbf{q}}\}\rangle, \tag{13}$$

$$|e_{\mathbf{q}}\rangle = |s_2\rangle |1_{\mathbf{q}}\rangle, \tag{14}$$

where $|s_1\rangle$ and $|s_2\rangle$ are eigenstates of σ_x ($\sigma_x|s_1\rangle = |s_1\rangle, \sigma_x|s_2\rangle = -|s_2\rangle$), $|\{0_{\mathbf{q}}\}\rangle$ stands for the vacuum state for phonon, and $|1_{\mathbf{q}}\rangle$ means that there is only one phonon for mode $\mathbf{q}$ and no phonon for other modes. Let $H'_1|g\rangle = 0$ and $\langle g|H'_2|g\rangle = 0$, we will get $\xi_{\mathbf{q}}$ and η, respectively, as follows:

$$\xi_{\mathbf{q}} = \frac{\omega_{\mathbf{q}}}{\omega_{\mathbf{q}} + 2\eta T_c}, \tag{15}$$

$$\eta = \exp\left(- \sum_{\mathbf{q}} \frac{|M_{\mathbf{q}}|^2}{2\omega^2_{\mathbf{q}}} \xi^2_{\mathbf{q}} \right). \tag{16}$$

Now we can easily check that $\langle e_s|H'_1|e_s\rangle = 0$, $\langle e_{\mathbf{q}}|H'_1|e_{\mathbf{q}}\rangle = 0$, $\langle e_s|H'_2|g\rangle = 0$, $\langle e_{\mathbf{q}}|H'_2|g\rangle = 0$, and $\langle e_{\mathbf{q}}|H'_1|e_s\rangle = V_{\mathbf{q}}$, where $V_{\mathbf{q}} = 2\eta T_c M_{\mathbf{q}} \xi_{\mathbf{q}} / \omega_{\mathbf{q}}$. With these relations above, we can now diagonalize the lowest excited states of H' as

$$H' = -\eta T_c |g\rangle\langle g| + \sum_E E|E\rangle\langle E| + \text{terms with high excited states}. \tag{17}$$

The experiment in Ref. 13 is performed at lattice temperature below 20 mK.[13,14] At such a low temperature, the multiphonon process is weak enough to be negligible. So we can get the transformation as[26–28]

$$|e_s\rangle = \sum_E x(E)|E\rangle, \tag{18}$$

$$|e_{\mathbf{q}}\rangle = \sum_E y_{\mathbf{q}}(E)|E\rangle, \tag{19}$$

$$|E\rangle = x(E)|e_s\rangle + \sum_{\mathbf{q}} y_{\mathbf{q}}(E)|e_{\mathbf{q}}\rangle, \tag{20}$$

where

$$|x(E)|^2 = \left(1 + \sum_{\mathbf{q}} \frac{|V_{\mathbf{q}}|^2}{(E + \eta T_c - \omega_{\mathbf{q}})^2} \right)^{-1}, \tag{21}$$

$$|y_{\mathbf{q}}(E)|^2 = \frac{|V_{\mathbf{q}}|^2}{(E + \eta T_c - \omega_{\mathbf{q}})^2} |x(E)|^2, \tag{22}$$

and the E's are solutions to the equation

$$E - \eta T_c - \sum_{\mathbf{q}} \frac{|V_{\mathbf{q}}|^2}{E + \eta T_c - \omega_{\mathbf{q}}} = 0. \tag{23}$$

The population inversion can be defined as $P(t) = \langle \psi(t)|\sigma_z|\psi(t)\rangle$, where $|\psi(t)\rangle$ is the total wave function (qubit and reservoir) in Schrödinger picture, and

$$|\psi(t)\rangle = e^{-S}e^{-iH't}e^{S}|\psi(0)\rangle. \tag{24}$$

Since the qubit is initially in the state $|L\rangle$, it is reasonable to choose $|\psi(0)\rangle = e^{-S}|L\rangle|\{0_{\mathbf{q}}\}\rangle$. Then we can obtain

$$\begin{aligned} P(t) &= \langle\{0_{\mathbf{q}}\}|\langle L|e^{iH't}e^{S}\sigma_z e^{-S}e^{-iH't}|L\rangle|\{0_{\mathbf{q}}\}\rangle \\ &= -\frac{1}{2}\sum_E |x(E)|^2 \exp[-i(E+\eta T_c)t] \\ &\quad -\frac{1}{2}\sum_E |x(E)|^2 \exp[i(E+\eta T_c)t] \\ &= -\frac{1}{4\pi i}\oint_C d\omega e^{-i\omega t}\left(\omega - 2\eta T_c - \sum_{\mathbf{q}} \frac{|V_{\mathbf{q}}|^2}{\omega + i0^+ - \omega_{\mathbf{q}}}\right)^{-1} \\ &\quad -\frac{1}{4\pi i}\oint_{C'} d\omega e^{i\omega t}\left(\omega - 2\eta T_c - \sum_{\mathbf{q}} \frac{|V_{\mathbf{q}}|^2}{\omega - i0^+ - \omega_{\mathbf{q}}}\right)^{-1}, \end{aligned} \tag{25}$$

where $\omega = E + \eta T_c$. Denoting the real and imaginary part of $\Sigma_{\mathbf{q}}|V_{\mathbf{q}}|^2/(\omega \pm i0^+ - \omega_{\mathbf{q}})$ as $R(\omega)$ and $\mp\gamma(\omega)$, respectively, we can get

$$\begin{aligned} R(\omega) &= \sum_{\mathbf{q}} \mathcal{P}\frac{|V_{\mathbf{q}}|^2}{\omega - \omega_{\mathbf{q}}} \\ &= 4(\eta T_c)^2 \mathcal{P}\int_0^\infty d\omega' \frac{J(\omega')}{(\omega - \omega')(\omega' + 2\eta T_c)^2}, \end{aligned} \tag{26}$$

$$\gamma(\omega) = \pi\sum_{\mathbf{q}} |V_{\mathbf{q}}|^2 \delta(\omega - \omega_{\mathbf{q}}) = 4\pi(\eta T_c)^2 \frac{J(\omega)}{(\omega + 2\eta T_c)^2}, \tag{27}$$

where $\mathcal{P}$ stands for Cauchy principal value, and the spectral density $J(\omega)$ is defined in Eq. (5). The parameter η determined by Eq. (15) and Eq. (16) can also be expressed as

$$\eta = \exp\left(-\int_0^\infty d\omega \frac{J(\omega)}{2(\omega + 2\eta T_c)^2}\right). \tag{28}$$

The contour integral in Eq. (26) can proceed by calculating the residue of integrand and the result is

$$P(t) = -\cos(\omega_r t)\exp(-\gamma t), \tag{29}$$

where we have applied the second order approximation,[26]

$$\gamma \simeq \gamma(2\eta T_c) = \tfrac{1}{4}\pi J(2\eta T_c), \tag{30}$$

and ω_r is the solution to the equation

$$\omega - 2\eta T_c - R(\omega) = 0. \tag{31}$$

Finally, the tunneling electron population (probablity) in the right dot at time t is given by

$$n(t) = \tfrac{1}{2}[1 + P(t)] = \tfrac{1}{2}[1 - \cos(\omega_r t)\exp(-\gamma t)]. \tag{32}$$

Thus a rather simple expression for the dynamical tunneling is obtained analytically. It should be noted here that our approach can be extended safely to strong coupling regime as compared to the previous work, since the perturbation H_1' and H_2' can be minimized by the variational parameter η. Also for this reason, it works well for the whole range of T_c if the system can be described by our Hamiltonian.

III. SPECTRAL DENSITY

The spectral density $J(\omega)$ defined by Eq. (5) is the only quantity describing the interaction between the system and its environment that enters into the dynamical tunneling. To get the final result, we need the knowledge of this spectral function first. Here, we only consider the coupling to the bulk acoustic phonons, because we are interested in low temperature limit. The only two types of interaction between electrons and acoustic phonons in semiconductors are piezoelectric coupling and deformation potential coupling. The piezoelectric coupling only presents in crystal lacking an inversion center. This is the case for III-V semiconductors such as GaAs (zinc-blende structure), although it is weak in comparison with II-VI materials.[30]

Take the electron wave functions $|L\rangle$ and $|R\rangle$ to be sharply around the center of left and right dot, respectively, with Gaussian shape $\sim\exp[-r^2/(2l^2)]$, where l is the dot size.[21] Assume the center-to-center distance d between two dots is sufficiently large as compared to l, so that wave functions $|L\rangle$ and $|R\rangle$ do not overlap significantly, i.e., the tunnel coupling between two dots is rather small, which is also complied with the experiment in Ref. 13, where the Rabi splitting due to interdot tuneling is about 10 μeV, while on-site charging energy is in the order of magnitude of meV. Then one can show that the piezoelectric coupling constant for GaAs is[20]

$$\begin{aligned} M_{\mathbf{q},\lambda}^{\mathrm{pz}} &= -\left(\frac{1}{2\rho q s_\lambda V}\right)^{1/2} M e^{-l^2q^2/4} \\ &\quad \times(\xi_1^\lambda e_2 e_3 + \xi_2^\lambda e_1 e_3 + \xi_3^\lambda e_1 e_2)\sin\left(\frac{\mathbf{q}\cdot\mathbf{d}}{2}\right), \end{aligned} \tag{33}$$

where ρ is the density of the crystal, V is the normalized volume, s is the sound velocity in crystal (longitudinal sound and transverse sound have different velocities), $e_i = q_i/q$, ξ is the polarization vector whose components depend on the polarization mode λ, and M is the piezoconstant. For a detailed derivation of this coupling constant see, e.g., Ref. 21. Here, we include the polarization again, since different polarization modes give different coupling constants. With the simple dispersion relation $\omega_{\mathbf{q},\lambda} = s_\lambda q$, one can now calculate the spectral function $J^{\mathrm{pz}}(\omega)$ due to piezoelectric coupling and obtain (in the spherical coordinate system)

$$J^{\mathrm{pz}}(\omega) = J_{\parallel}^{\mathrm{pz}}(\omega) + J_{\perp 1}^{\mathrm{pz}}(\omega) + J_{\perp 2}^{\mathrm{pz}}(\omega), \tag{34}$$

where

$$J_{\parallel}^{\mathrm{pz}}(\omega)=\frac{M^2}{\pi^3\rho s^3}\omega e^{-\omega^2/2\omega_l^2}\int\int(3\sin^2\theta\cos\theta\sin\phi\cos\phi)^2\times\sin^2\left(\frac{\omega}{\omega_d}\cos\theta\right)\sin\theta d\theta d\phi, \tag{35}$$

$$J_{\perp 1}^{\mathrm{pz}}(\omega)=\frac{M^2}{\pi^3 x\rho s^3}\omega e^{-\omega^2/2\omega_l^2}\int\int[\sin\theta\cos\theta(\sin^2\phi-\cos^2\phi)]^2\sin^2\left(\frac{\omega}{\omega_d}\cos\theta\right)\sin\theta d\theta d\phi, \tag{36}$$

$$J_{\perp 2}^{\mathrm{pz}}(\omega)=\frac{M^2}{\pi^3 x\rho s^3}\omega e^{-\omega^2/2\omega_l^2}\int\int(\sin^3\theta\sin\phi\cos\phi-2\sin\theta\cos^2\theta\sin\phi\cos\phi)^2\times\sin^2\left(\frac{\omega}{\omega_d}\cos\theta\right)\sin\theta d\theta d\phi, \tag{37}$$

where $\omega_d=s/d$, $\omega_l=s/l$, and x is the ratio of transverse velocity to longitudinal velocity. Most many-body calculations take an angular average for the sake of analytical simplicity, and it involves only minor quantitative differences.[29,30] To obtain a tractable form of the piezoelectric coupling we also adopt this approximation, that is

$$\sin^2\left(\frac{\omega}{\omega_d}\cos\theta\right)\rightarrow\frac{\int\int\sin^2\left(\frac{\omega}{\omega_d}\cos\theta\right)\sin\theta d\theta d\phi}{\int\int\sin\theta d\theta d\phi}=\frac{1}{2}\left(1-\frac{\omega_d}{\omega}\sin\frac{\omega}{\omega_d}\right). \tag{38}$$

Then we get

$$J^{\mathrm{pz}}(\omega)=g_{\mathrm{pz}}\omega\left(1-\frac{\omega_d}{\omega}\sin\frac{\omega}{\omega_d}\right)e^{-\omega^2/2\omega_l^2}, \tag{39}$$

where

$$g_{\mathrm{pz}}=\frac{M^2}{\pi^2\rho s^3}\left(\frac{6}{35}+\frac{1}{x}\frac{8}{35}\right). \tag{40}$$

For the deformation potential coupling, the contribution from TA-acoustic phonons is small enough to be neglected as compared with that from LA-acoustic phonons. So the coupling constant can be written as[20]

$$M_{\mathbf{q}}^{\mathrm{df}}=iq\Xi\left(\frac{1}{2\rho qsV}\right)^{1/2}e^{-l^2q^2/4}\sin\left(\frac{\mathbf{q}\cdot\mathbf{d}}{2}\right), \tag{41}$$

where Ξ is the deformation potential. Then we can easily get the spectral function due to deformation coupling

$$J^{\mathrm{df}}(\omega)=g_{\mathrm{df}}\omega^3\left(1-\frac{\omega_d}{\omega}\sin\frac{\omega}{\omega_d}\right)e^{-\omega^2/2\omega_l^2}, \tag{42}$$

where $g_{\mathrm{df}}=\Xi^2/8\pi^2\rho s^5$.

With the parameters of GaAs in Ref. 30, we can estimate that $g_{\mathrm{pz}}\approx 0.035$ and $g_{\mathrm{df}}\approx 0.029$ $(\mathrm{ps})^{-2}$. Previous work states that the contribution from deformation potential phonons is small as compared with piezoelectric phonons in double-dot system of GaAs material.[22] Our result also proves it to be true in the weak confinement regime (large dot). But it is not valid in the strong confinement regime (small dot). Figure 1 shows the spectral functions $J^{\mathrm{pz}}(\omega)$ and $J^{\mathrm{df}}(\omega)$ in strong confinement regime, with $\omega_l=1$ $(\mathrm{ps})^{-1}$ (i.e., dot size $l=5$ nm) and $\omega_l=0.5$ $(\mathrm{ps})^{-1}$ (i.e., dot size $l=10$ nm). As we can see, $J^{\mathrm{df}}(\omega)$ is comparable to $J^{\mathrm{pz}}(\omega)$ in that regime. But $J^{\mathrm{df}}(\omega)$ shrinks much faster than $J^{\mathrm{pz}}(\omega)$ as the dot size is increased and is negligible when the dot size $l>50$ nm. Figure 1 also shows the spectral functions $J^{\mathrm{pz}}(\omega)$ and $J^{\mathrm{df}}(\omega)$ at two different center-to-center distances, with $\omega_d=0.05$ $(\mathrm{ps})^{-1}$ (i.e., $d=100$ nm) and $\omega_d=0.02$ $(\mathrm{ps})^{-1}$ (i.e., $d=250$ nm). The influence from the parameter d to both $J^{\mathrm{pz}}(\omega)$ and $J^{\mathrm{df}}(\omega)$ is small as compared with that from the parameter l. It adds an oscillation term to the spectral function, and the oscillation frequency (determined by ω_d) is increased with d. All these properties of spectral functions $J^{\mathrm{pz}}(\omega)$ and $J^{\mathrm{df}}(\omega)$ determine the decoherence induced by piezoelectric coupling and deformation potential coupling to phonons, respectively.

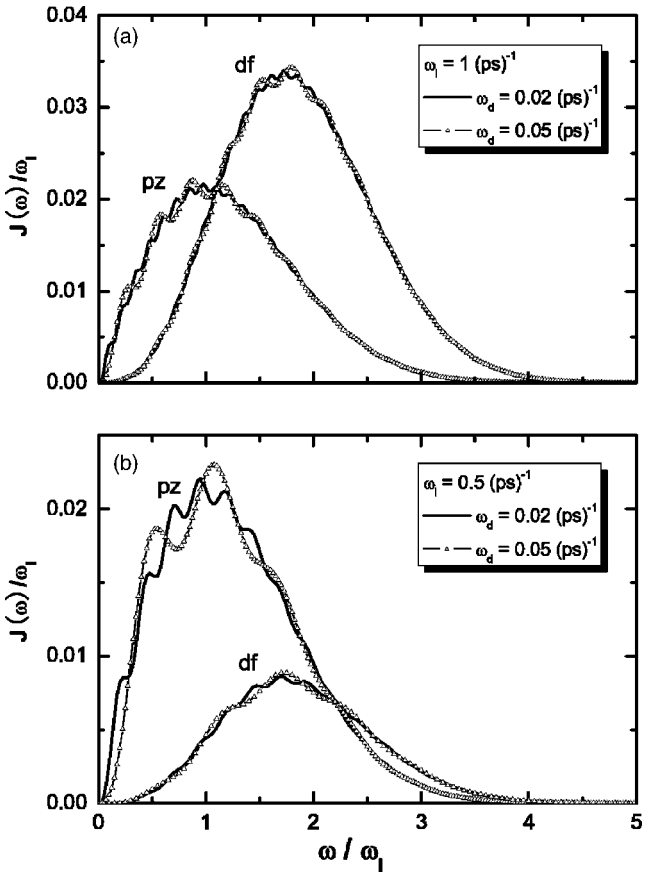

FIG. 1. Spectral functions of double quantum dot due to piezoelectric coupling (labeled by pz) and deformation potential coupling (labeled by df) with $\omega_d=0.02$ and $\omega_d=0.05$ $(\mathrm{ps})^{-1}$. (a) $\omega_l=1$ $(\mathrm{ps})^{-1}$. (b) $\omega_l=0.5$ $(\mathrm{ps})^{-1}$.

As one can see in Eq. (33) and Eq. (41), the deformation potential coupling constant is imaginary, while the piezoelectric coupling constant is real, which means they do not interfere with each other.[29,30] Thus the total spectral density is

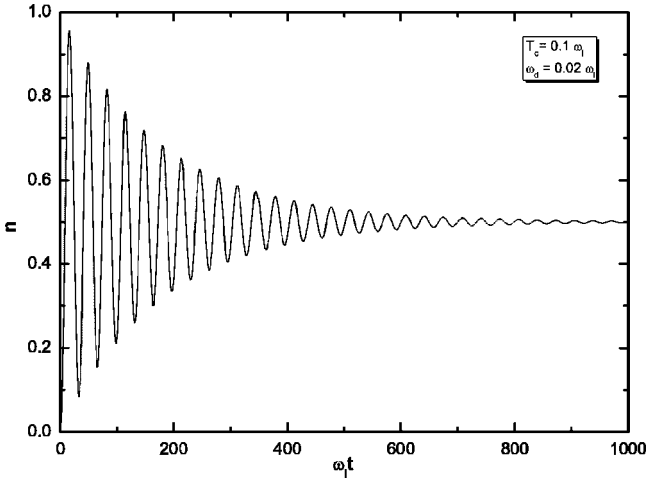

FIG. 2. The tunneling electron population in the right dot as a function of $\omega_l t$ for GaAs double quantum dot with $T_c = 0.1\omega_l$ and $\omega_d = 0.02\omega_l$.

$$J(\omega) = J^{\mathrm{pz}}(\omega) + J^{\mathrm{df}}(\omega). \tag{43}$$

Since now we have the knowledge of the spectral function, it is easy to get the dynamics of the tunneling electron in DQD system, as shown in Fig. 2. The damped oscillation form is agreed with the result of the experiment.[13]

IV. PHONON INDUCED DECOHERENCE

The decoherence of quantum system due to the interaction with environment is a crucial point in quantum information. In a double quantum dot, scattering by phonons can cause considerable loss of coherence accompanied by dissipation when the tunneling electron flips back and forth between two dots. One of the advantages of our approach is that the decoherence rate in this process is obtained explicitly. Thus one can analyze it clearly.

Using the expressions of spectral density $J^{\mathrm{pz}}(\omega)$ [Eq. (39)] and $J^{\mathrm{df}}(\omega)$ [Eq. (42)] above, the decoherence rates induced by piezoelectric and deformation potential coupling are written as

$$\gamma_{\mathrm{pz}} = \frac{1}{2}\pi g_{\mathrm{pz}} \eta T_c \left(1 - \frac{\omega_d}{2\eta T_c} \sin \frac{2\eta T_c}{\omega_d}\right) e^{-2\eta^2 {T_c}^2/{\omega_l}^2}, \tag{44}$$

and

$$\gamma_{\mathrm{df}} = 2\pi g_{\mathrm{df}} \eta^3 {T_c}^3 \left(1 - \frac{\omega_d}{2\eta T_c} \sin \frac{2\eta T_c}{\omega_d}\right) e^{-2\eta^2 {T_c}^2/{\omega_l}^2}, \tag{45}$$

respectively. Here it should be noted that the parameter η in Eq. (44) and Eq. (45) are not the same, because they are calculated from Eq. (28) with different spectral functions [$J^{\mathrm{pz}}(\omega)$ and $J^{\mathrm{df}}(\omega)$, respectively]. According to Eq. (43), the total decoherence rate induced by acoustic phonons is $\gamma = \gamma_{\mathrm{pz}} + \gamma_{\mathrm{df}}$.

Figure 3 presents the decoherence rates γ_{pz} and γ_{df} as functions of ω_l at two different tunneling rates

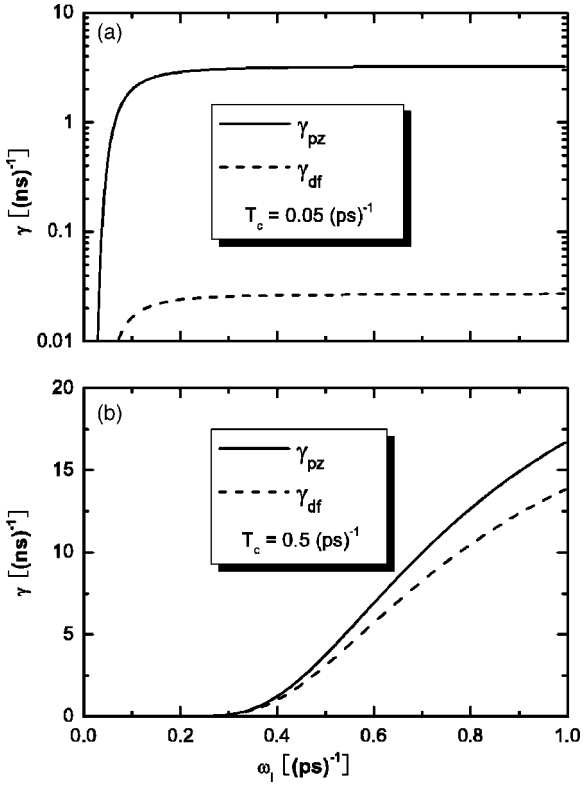

FIG. 3. Decoherence rates γ_{pz} (solid line) and γ_{df} (dashed line) as functions of cutoff frequency ω_l when $\omega_d = 0.02\ (\mathrm{ps})^{-1}$. The tunneling rates in (a) and (b) are $0.05\ (\mathrm{ps})^{-1}$ and $0.5\ (\mathrm{ps})^{-1}$, respectively.

$T_c = 0.05\ (\mathrm{ps})^{-1}$ and $T_c = 0.5\ (\mathrm{ps})^{-1}$. Another parameter ω_d is fixed as $0.02\ (\mathrm{ps})^{-1}$, which means the center-to-center distance between two dots is about 250 nm. As shown in Fig. 3(a), at small tunneling rate, the contribution to decoherence rate caused by deformation potential coupling is small as compared with that from piezoelectric coupling, even in strong confinement regime [i.e., $\omega_l \sim 1\ (\mathrm{ps})^{-1}$]. But when the tunneling rate is large [Fig. 3(b)], the decoherence rates arising from these two mechanisms are comparable, thus the contribution from the deformation potential coupling cannot be neglected in such a situation. Figures 3(a) and 3(b) also show that the decoherence rates (both γ_{pz} and γ_{df}) are suppressed when ω_l is decreased, which indicates that one should use large dot size to get small decoherence. However, large dot size means small characteristic energy spacing (on-site charging energy) ω_{01} of single quantum dot. It is well known that, our two-level Hamiltonian is valid to describe the double-dot system only if T_c, $k_B T \ll \omega_{01}$, where k_B is Boltzmann constant.[31] Therefore, the low temperature technique is needed to maintain good quantum properties of dots when the dot size is large, just as the experiment is performed.[13]

In what follows, we choose a large dot size of 100 nm (approximate size for the dot in Ref. 13), i.e., $\omega_l = 0.05\ (\mathrm{ps})^{-1}$. Since the tunneling barriers in experiment of Ref. 13 are made by depleting electrons with negative gate voltage, their tunneling rates are flexible.[32] In Fig. 4, we present the decoherence rate γ ($\approx \gamma_{\mathrm{pz}}$ at that dot size) as a

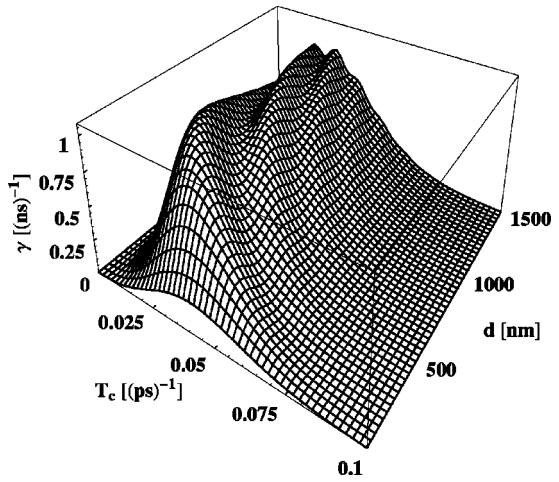

FIG. 4. Decoherence rate γ as a function of tunneling rate T_c and distance d between two dots. The dot size is chosen to be 100 nm.

function of tunneling rate and distance between two dots (from 100 to 1500 nm). Some oscillations due to the sine term in the spectral density are demonstrated from this three-dimensional figure. We find that the characteristic decoherence time $T_2=1/\gamma$ speculated from the figure is about 1 ns, which agrees well with the value fitted from the experimental curve.[13] So the coupling to phonons is one of the main decoherence mechanisms in such a double-dot system. It also shows that the decoherence rate increases with tunneling rate T_c when $T_c<\omega_l$. But larger tunneling rate will suppress the decoherence drastically, even to zero when $T_c\approx 0.1$ $(\mathrm{ps})^{-1}$ (i.e., $2\omega_l$). This value of T_c is still in the range of $\ll\omega_{01}=1.3$ meV ~ 2 $(\mathrm{ps})^{-1}$,[13] in which our two-level model holds. Thus, such kind of decoupling mechanism can be probably realized.

V. CONCLUSION

In conclusion, we have investigated the charge qubit dynamics in a semiconductor double quantum dot coupled to phonons at low temperature limit. Our approach is a perturbation theory after a unitary transformation. The dynamical tunneling current is obtained explicitly as a simple damped Rabi oscillation. Compared to the previous work our approach is not restricted by the form of spectral density and can be extended to strong coupling regime and works well for the whole range of tunneling rate T_c. Additionally, a simple expression for the decoherence rate allows us to analyze the phonon induced decoherence clearly. We find that, in strong confinement regime of dot and large tunneling rate T_c $[>0.1$ $(\mathrm{ps})^{-1}]$, the contribution to decoherence from deformation potential coupling cannot be neglected as compared to that from piezoelectric coupling in GaAs material. The decoherence arising from both these two mechanisms will be suppressed when the dot size is increased. The decoupling with phonons will happen when the condition $2\omega_l<T_c\ll\omega_{01}$ is satisfied. Finally, we hope that our predictions can be testified by experiment in the near future.

ACKNOWLEDGMENTS

The authors thank T. Fujisawa for helpful discussions and careful reading of this paper. This work was partly supported by National Natural Science Foundation of China (Grant No. 10274051) and Shanghai Natural Science Foundation (Grant No. 03ZR14060).

*Electronic address: wuzj@sjtu.edu.cn

[1] D. Bouwmeester, A. K. Ekert, and A. Zeilinger, *The Physics of Quantum Information* (Springer-Verlag, Berlin, 2000).
[2] M. A. Nielsen and I. L. Chuang, *Quantum Computation and Quantum Information* (Cambridge University Press, United Kingdom, 2000).
[3] C. Monroe, Nature (London) **416**, 238 (2002).
[4] D. Loss and D. P. DiVincenzo, Phys. Rev. A **57**, 120 (1998).
[5] B. E. Kane, Nature (London) **393**, 133 (1998).
[6] Y. Nakamura, Yu. A. Pashkin, and J. S. Tsai, Nature (London) **398**, 786 (1999).
[7] E. Bibow, P. Lafarge. and L. P. Levy, Phys. Rev. Lett. **88**, 017003 (2001).
[8] A. Zrenner, E. Beham, S. Stufler, F. Findeis, M. Bichler, and G. Abstreiter, Nature (London) **418**, 612 (2002).
[9] T. Fujisawa, T. H. Oosterkamp, W. G. van der Wiel, B. W. Broer, R. Aguado, S. Tarccha, and L. P. Kouwenhoven, Science **282**, 932 (1998).
[10] T. H. Oosterkamp, T. Fujisawa, W. G. van der Wiel, K. Ishibashi, R. V. Hijman, S. Tarucha, and L. P. Kouwenhoven, Nature (London) **395**, 873 (1998).
[11] S. Gardelis, C. G. Smith, J. Cooper, D. A. Ritchie, E. H. Linfield, Y. Jin, and M. Pepper, Phys. Rev. B **67**, 073302 (2003).
[12] L. C. L. Hollenberg, A. S. Dzurak, C. Wellard, A. R. Hamilton, D. J. Reilly, G. J. Milburn, and R. G. Clark, Phys. Rev. B **69**, 113301 (2004).
[13] T. Hayashi, T. Fujisawa, H. D. Cheong, Y. H. Jeong, and Y. Hirayama, Phys. Rev. Lett. **91**, 226804 (2003).
[14] T. Fujisawa, T. Hayashi, and Y. Hirayama, J. Vac. Sci. Technol. B **22**, 4 (2004).
[15] T. Brandes and B. Kramer, Phys. Rev. Lett. **83**, 3021 (1999).
[16] T. Brandes and T. Vorrath, Phys. Rev. B **66**, 075341 (2002).
[17] R. Aguado and T. Brandes, Eur. Phys. J. B **40**, 357 (2004).
[18] R. Aguado and T. Brandes, Phys. Rev. Lett. **92**, 206601 (2004).
[19] T. Brandes, R. Aguado, and G. Platero, Phys. Rev. B **69**, 205326 (2004).
[20] L. Fedichkin and A. Fedorov, Phys. Rev. A **69**, 032311 (2004).
[21] L. Fedichkin and A. Fedorov, Nanotechnology **4**, 65 (2005).
[22] T. Brandes, Phys. Rep. **408**, 314 (2005).
[23] A. J. Leggett, S. Chakravarty, A. T. Dorsey, M. P. A. Fisher, A. Garg, and W. Zwerger, Rev. Mod. Phys. **59**, 1 (1987).
[24] U. Weiss, *Quantum Dissipative System* (World Scientific, Singapore, 1993).
[25] R. Silbey and R. A. Schoeller, J. Chem. Phys. **80**, 2615 (1984).

[26] H. Zheng, Eur. Phys. J. B **38**, 559 (2004).
[27] Z.-J. Wu, K.-D. Zhu, and H. Zheng, Phys. Lett. A **333**, 310 (2004).
[28] F. Guinea, V. Hakim, and A. Muramatsu, Phys. Rev. B **32**, 4410 (1985).
[29] H. Bruus, K. Flensberg, and H. Smith, Phys. Rev. B **48**, 11 144 (1993).
[30] G. D. Mahan, *Many-Particle Physics* (Plenum, New York, 1990).
[31] S. D. Barrett and G. J. Milburn, Phys. Rev. B **68**, 155307 (2003).
[32] T. Fujisawa (private communication).